Output Power Saturation with a Discharge Current in Powerful Continuous Argon Lasers

V. I. Donin
Institute of Semiconductor Physics, Siberian Division, USSR Academy of Sciences
Submitted October 21, 1971
Zh. Eksp. Teor. Fiz. 62, 1648–1660 (May, 1972)

The electric and optical parameters of an argon plasma in a high current discharge in large diameter tubes ($\gtrsim 10$ mm) are investigated with the purpose of explaining generation saturation with a pumping current in powerful continuous ion lasers. It is found that the decrease of the gas atom concentration N in the discharge on increase of the pumping current considerably affects the plasma parameters and the operation of the ion laser. The results show that generation saturation, just as in the small diameter tubes previously studied, is due to restriction of the excitation rate of the working levels resulting from a sharp decrease of N in the discharge occurring at saturating currents. In a tube of 16 mm diameter and an active length of 135 cm the output power under saturation conditions is 175 W.

INTRODUCTION

A laser using ArII ions is at the present time the most powerful source of continuous coherent radiation in the visible region of the spectrum. The most important question in this connection is that of the saturation of the output power of an argon laser when the discharge current is increased, since this saturation determines the maximum obtainable generation power and the efficiency of the argon laser. Investigations performed with small-diameter discharge tubes ($\lesssim 3$ mm) have shown that the saturation of the generation power with increasing discharge current in such tubes is connected with the saturation of the rate of excitation of the working levels as the result of a decrease in the concentration of the working-gas atoms in the discharge[1]. The presently available experimental data on argon lasers in the current-saturation regime, for large-diameter tubes ($\gtrsim 10$ mm) are confined to the dependences of the generation power and of the maintaining voltage on the discharge current at different gas pressures[2-4], and to the influence of an external magnetic field on the generation power and on the maintaining voltage[2]. As noted earlier[2], the behavior of the generation power and the maintaining voltage as functions of the discharge current in wide tubes agrees qualitatively with their behavior in tubes having a small diameter only at low gas pressures, and a difference appears at higher pressures. This circumstance, and also the total absence of experimental data on the parameters of a strong-current continuous discharge plasma at low pressure in large-diameter tubes, makes it unclear whether the saturation of the generation as a function of the current discharge at higher pressures is due to a decrease in the concentration of the atoms in the discharge or whether it stems from another source. Interest in the problem of saturation in wide tubes is further increased by the larger output power per unit discharge length, obtained from such tubes because of the large cross-section area.

Our present paper is devoted to an experimental study of the electric and optical characteristics of a strong-current discharge plasma of reduced pressure in large-diameter tubes, to a discussion of the influence of the plasma characteristics on the operation of an argon laser, and to an explanation of the saturation of the output power with increasing discharge current.

EXPERIMENTAL PROCEDURE AND PRINCIPAL RESULTS

The investigated argon plasma was produced by a high-power DC discharge in a tube consisting of individual water-cooled aluminum sections coated with a dielectric Al_2O_3 film. Such tubes, intended for operation at lower discharge currents, were described earlier[5,6]. The structural modification made in our tube were aimed at increasing the discharge current and will be described elsewhere. Each section was 2 cm long, the distance between them was ~ 0.5 mm and the vacuum seals were teflon gaskets. High electron emission in the discharge was ensured by using a cold arc cathode[7]. The electrodes were made coaxial with the discharge tube. Most of the results were obtained with a tube having a discharge channel of 11 mm diameter and 50 cm length. Since the discharge channel broadened gradually towards the electrodes, the effective active length of the discharge, l, was larger and amounted to ~ 55 cm. The discharge tube was mounted on a special stage that could be moved laterally relative to the tube axis. To eliminate the influence of electrophoresis, additional channels joining the anode and cathode regions of the discharge were provided in addition to the discharge channel. The gas pressure was measured in the cold part of the tube. The tube was fed from a rectifier with a three-phase bridge rectification circuit, and the discharge current was regulated with ballast resistors. Figure 1 shows a diagram of the experimental setup for the measurement of the spectral characteristics of the plasma. The spontaneous emission from the discharge, after passing through diaphragms D_1 and D_2 of 1 mm diameter, an interferometer with a lens, and a three-prism spectrograph (linear dispersion 3 Å/mm in the spectral region 4500 Å), was registered with the aid of a photomultiplier. The spectral line contours were recorded by displacing one of the interferometer mirrors with a piezoceramic. The piezoceramic was fed from a sawtooth voltage generator. The interferometer mirrors had high-reflectivity dielectric coatings, and the base of the interferometer was chosen to suit the width of the investigated line. The contours were obtained for the hydrogen H_α and H_β lines (the hydrogen was present in the discharge in the form of a slight impurity), the

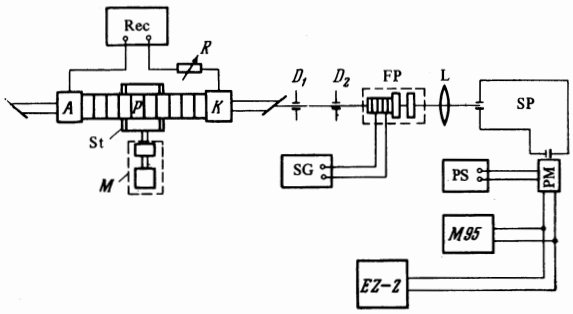

FIG. 1. Setup for the measurement of plasma spectral characteristics. P–discharge tube, A and K–anode and cathode discharge tube, Rec–rectifier, R–balast resistor, St–moving stage, M–electric motor and reduction gear, D_1 and D_2–diaphragms, FP–scanned Fabry-Perot interferometer, SG–sawtooth voltage generator, L–lens, SP–spectrograph, PM–photomultiplier, PS–power supply for photomultiplier, M95–galvinometer, EZ-2–automatic recorder.

atomic argon line with emission wavelength $\lambda = 4200.7$ Å, and the lines $\lambda = 4880$ Å and $\lambda = 5145$ Å of singly-ionized argon. To record the contours of the ArII lines, the radiation was extracted perpendicular to the tube axis, through a lateral hole of 2 mm diameter cut in one of the sections and sealed with a glass window.

The electron concentration n_e was determined from the Stark broadening of the H_β line. Under the experimental conditions, the Doppler width of this line was comparable with the Stark width. The simplify the separation of the Stark broadening from the Doppler broadening, it was assumed that the Stark contour of H_β is described by the Lorentz formula. This has made it possible to separate the Stark line width from the measured width by using the known tables for the Voigt spectral line contours. The Doppler width of the H_β line was calculated from the known temperature gas T_a as measured by determining the broadening of the H_α line, which was governed by the Doppler effect under the experimental conditions. The obtained values of n_e on the discharge axis for an argon pressure 0.65 mm Hg are shown in Fig. 2. The figure shows also the values of T_a obtained from measurements of the H_α line and of the atomic argon line. We see that the difference between the values of T_a determined from the hydrogen and the argon lines increases with increasing discharge current. Even if we assume, when determining n_e from the H_β line, that the Doppler width of the latter is determined by a temperature that coincides with that determined from the Ar I line, the general form of the n_e curve remains unchanged (curve 3′). Thus, the general character of the variation of n_e with changing discharge current can be assumed to be reliably established. The accuracy with which the absolute value of n_e is determined is not high (±50%) and is governed mainly by the considerable influence of the Doppler broadening on the contour of the H_β line. The current dependence of the ion temperature T_i, determined from the Ar II lines measured at the end of the tube, is well approximated in the current range 150–300 A by curve 1 of Fig. 2, but T_i has a noticeable tendency to decrease above 300 A. The ion temperature T_i measured from the side of the tube also increased with the current and amounted to 1.8×10^4°K at 300 A.

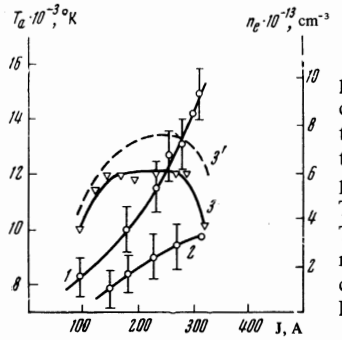

FIG. 2. Values of the atom temperature (T_a) and of the electron concentration (n_e) on the axis of a tube of 11 mm diameter as functions of the discharge current J. Gas pressure p = 0.65 mm Hg. Curve 1–T_a obtained from the H_α line, 2–T_a from the ArI 4200.7 Å line, 3–n_e obtained from the H_β line using curve 1, 3′–n_e obtained from the H_β line using curve 2.

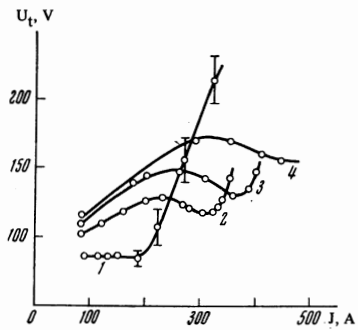

FIG. 3. Current-voltage characteristics of the discharge at p = 0.25 mm Hg (curve 1), p = 0.65 mm Hg (curve 2), p = 1 mm Hg (curve 3), p = 1.3 mm Hg (curve 4).

Figure 3 shows the change of the tube voltage U_t with changing discharge currents for different gas pressures. U_t was measured directly between the outermost sections of the discharge tube, i.e., not including the anode and cathode voltage drops. The voltage drop across the active length of the tube is approximately 25% smaller than U_t, owing to the presence of the already-mentioned expanding transition regions of the discharge. As seen from Fig. 3, each plot of the voltage against the current has a minimum followed by a very sharp rise. In the sections where the voltage has the sharp rise, the experimental points have a considerable scatter, which is shown for curve 1. Oscillograms of the voltage U_L between two neighboring sections (the variation of U_L with current was analogous to the variation of U_t) have shown that, starting with the instant when the maintaining voltage reaches a minimum, strong noise-like voltage oscillations followed the increase of the discharge current and were accompanied by increased erosion of the discharge-tube wall and by an impurity content of the discharge, particularly hydrogen. These oscillations differ from the oscillations that occur when the pressure is increased, for in the latter case there was no damage to the tube even in the case of currents several times larger than the indicated ones.

By moving the discharge tube uniformly parallel to the axis in horizontal plane, with the aid of an electric motor, it was possible to obtain the distribution of the spontaneous-emission intensity over the tube cross-section. The tube was moved rather than the diaphragms, in order to maintain a constant angle between the radiation and the axis of the optical system. We plotted the radial distribution of the radiation of the Ar II 4880 and 5145 Å lines and of the Ar I 4198 and 4259 Å lines. The distribution of the radiation for both

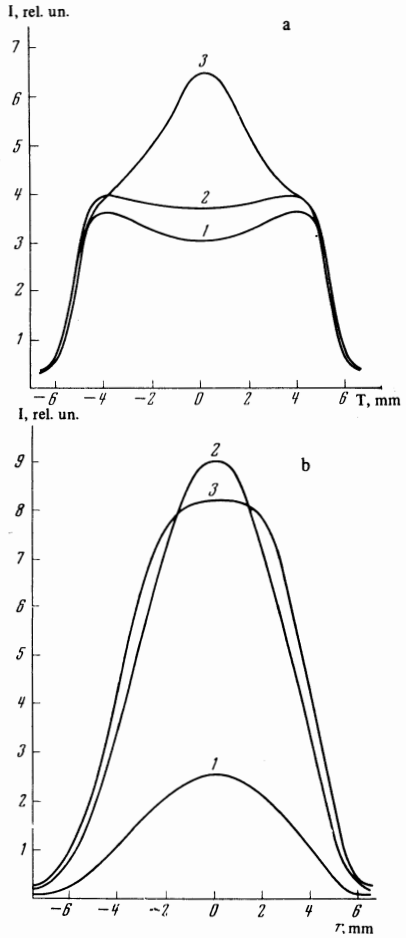

FIG. 4. Spontaneous-emission intensity I as a function of the distance to the tube axis r at p = 0.65 mm Hg. a–ArI 4198 Å line 5p [1/2] –4s [3/2]^0, curves 1, 2, and 3 correspond to currents 110, 200, and 280 Å; b–ArII 4880 Å line, $4p^2D_{5/2}{}^0$–$4s^2P_{3/2}$, curves 1, 2, and 3 correspond to currents 110, 220, and 300 Å.

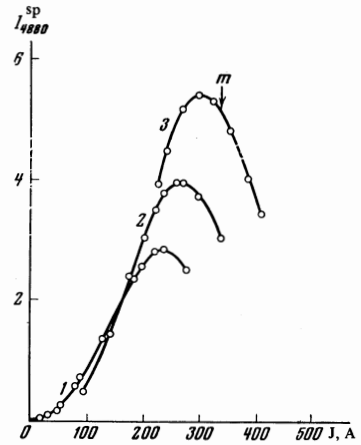

FIG. 5. Spontaneous-emission intensity I integrated over the discharge cross section of the 4880 Å line (in relative units) as a function of J for p = 0.3 mm Hg (curve 1), p = 0.65 mm Hg (curve 2), and p = 1 mm Hg (curve 3).

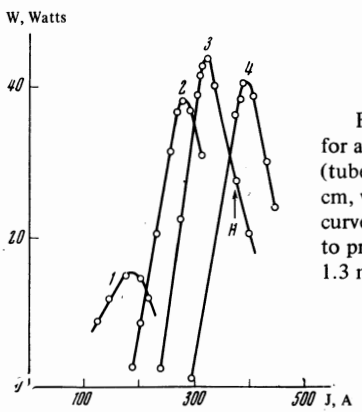

FIG. 6. Generation power W for all lines, as a function of j (tube of 11 mm diameter, l = 55 cm, with quartz output windows); curves 1, 2, 3, and 4 correspond to pressures 0.25, 0.65, 1, and 1.3 mm Hg.

atomic lines was practically the same, as illustrated in Fig. 4a. The ionic lines had a similar radial distribution (Fig. 4b). Self-absorption of the radiation changed the line intensity not more than 12% under the measurement conditions. The reabsorption of the atomic lines was monitored with a mirror behind the discharge[8] and depended little on the current. The intensity of the spontaneous emission from the entire cross section of the discharge is shown in Fig. 5 for the 4880 Å ion line, which had the largest gain of all the generated lines. In this case the measurements were made without the diaphragms and the interferometer with the lens. At a discharge current 280 A and at a pressure 0.65 mm Hg, the absolute intensity of the spontaneous emission on the discharge axis was measured for the Ar II lines observed in the generation, using a standard procedure with a tungsten ribbon lamp calibrated to a color temperature 2360°K. If it is assumed that the disintegration of the upper working levels is due only to spontaneous emission, then the level population can be determined from the known emission intensities and transition probabilities[9]. For the 4880 Å line, the upper-level population obtained in this manner at the center of the tube amounted to $(1.8 \pm 0.2) \times 10^{10}$ cm^{-3}. Since the absolute level population was measured under discharge conditions close to optimal for lasing, the measurements for the 4880 Å line were corrected for negative absorption of [illegible] radiation (~ 12%) using the known optical density $\kappa_0 l = 0.36$, which was obtained by introducing calibrated losses into the laser resonator. The laser consisted of the indicated discharge tube and two dielectric mirrors for the blue-green part of the spectrum, each with a curvature radius R = 6 m and transmission T ~ 2%, spaced 1.8 m apart. The laser was also used to plot the generation power against the current, as shown in Fig. 6. The absolute values of the output power were measured by a calorimetric method with an error ±10%.

Analogous plots of the output power against the discharge current were obtained with another tube of 16 mm diameter and active length 135 cm. The resonator consisted in this case of two internal mirrors with R = 10 m and transmissions T = 2 and 2.5%, respectively, for the strongest generation lines λ = 5145 Å and λ = 4880 Å. Figure 7 shows the current dependence of the generation power in this tube at near-optimal pressure. The figure shows also the values of the tube voltage, which is close in this case to the voltage drop across the active length of the tube.

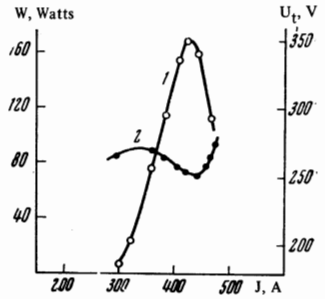

FIG. 7. Dependence of the generation power W (curve 1) and of the tube voltage U_t (curve 2) on J in a tube of 16 mm diameter and l = 135 cm, with internal mirrors; p = 0.7 mm Hg.

DISCUSSION OF RESULTS

1. Electrical Characteristics of the Plasma

The plot of the electron concentration against the discharge current J (Fig. 2) shows saturation at $J \gtrsim 150$ A. Since the current in the discharge is due in practice to the motion of the electrons, it is obvious that further increase of the current is connected with an increase in the translational velocity of the electrons, which is an increasing function of the parameter E/p_0[10], where E is the intensity of the longitudinal electric field and p_0 is the relative pressure of the gas. It is seen from Fig. 3 that if the gas pressure in the cold part is p = 0.65 mm Hg, the field intensity decreases, starting with J = 200—250 A, and consequently the increase of the electron drift velocity is due to the appreciable decrease of the gas pressure in the discharge. Let us consider the dependence of the voltage in the discharge on the current; this dependence of determined by the electric conductivity σ of the plasma. The expression for σ is derived in the general case on the basis of a solution of the Boltzmann kinetic equation and takes the form[11]

$$\sigma = \frac{j}{E} = K_\sigma^{(n)} \frac{e^2 n_e}{m_e \nu_a (1+P)} = K_\sigma^{(n)} \frac{e^2 n_e}{m_e \bar{v} [\langle Q_a \rangle N_a + \langle Q_i \rangle N_i]} \quad (1)$$

where the following notation is used: p, m_e, and $\bar{v}$ are respectively the charge, mass, and average velocity of the electron; $P = \nu_i/\nu_a = \langle Q_i \rangle N_i \bar{v} / \langle Q_a \rangle N_a \bar{v}$ is the ratio of the effective electron-ion collision frequency to the effective electron-atom collision frequency; N_i and N_a are the concentrations of the ions and the atoms; $\langle Q_i \rangle$ and $\langle Q_a \rangle$ are the corresponding effective interaction of the electrons with the ions and with the atoms (the electric-conductivity cross sections). The electron-electron collisions are included in the kinetic coefficient $K_\sigma^{(n)}$, where the superscript denotes the n-th approximation when σ is determined by the Chapman-Enskog method; the values of the kinetic coefficient for argon are given in[12]. As seen from Figs. 2 and 3, the concentration of the charge particles remains unchanged in the region of negative slope, and therefore, according to (1), the main factor governing the sharp increase of σ with increasing J is the decrease of N_a. Some contribution can be made also by $\langle Q_i \rangle$ and $\langle Q_a \rangle$, owing to their dependence on the electron temperature.[13] The values of $K_\sigma^{(n)}$ and $\bar{v}$ vary slowly and cancel each other[1)]. The succeeding transition to a positive current-voltage characteristic with a steep rise of the voltage and with the onset of oscillations can be naturally attributed to the appearance of nonlinear effects in the plasma, and an additional cause of the voltage rise may be the increase of the impurity content in the discharge and the decrease of n_e. The onset of instabilities in the plasma can greatly complicate the interpretation of the occurring phenomena; for example, the instabilities can cause charged particles to escape from the discharge. In our case, however, when we consider the saturation of the generation with increasing discharge current, the instabilities can be disregarded, for it is seen from Figs. 3 and 6 that with increasing current the generation saturates long before the instabilities occur (for clarity, the arrow in Fig. 6 marks the onset of instabilities in the case of p = 1 mm Hg).

The decrease of N_a in the discharge with increasing J can lead to an increase in the degree of ionization of the gas and to a rise in the electron temperature T_e, since the latter is inversely proportional to the pressure p_0[10]. As can be seen from Fig. 2, at currents $\lesssim 150$ A, the degree of ionization is increased simultaneously as a result of the increase of n_e and the decrease of N_a, and at higher currents it increases only as the result of the decrease of N_a. The increase of the degree of ionization of the gas, due to the decrease of N_a without an increase of n_e in an argon-laser plasma operating in the current saturation regime, was already pointed out in[1], where it was noted that the degree of ionization of the gas in the axial part of the discharge is extremely high for continuous discharges. The decrease of N_a in the discharge with increasing J may be due to the following factors. First, when J is increased the temperature of all the particles in the plasma rises, and this should cause N_a to be crowded out of the discharge, especially out of its axial parts. Second, under discharge conditions characteristic of the argon laser operation, the mean free path of the atoms is comparable with the tube radius r[13], and therefore the time of flight of the atoms will be $\tau_f \sim r/\bar{v}_a$, where $\bar{v}_a$ is the average thermal velocity of the atoms. It is easy to see that at argon ionization cross sections $\langle q_i \rangle \sim 10^{-16}$ cm^2[14,10] the ionization time of the atom is $\tau_i \sim (n_e \bar{v} \langle q_i \rangle)^{-1}$, and under the conditions in question is comparable with τ_f, i.e. the atom has time to become ionized during the time it traverses the radius of the tube and is removed, in the form of an ion, from the discharge at the walls. This should also lead to a decrease of N_a on the discharge axis. The influence of the ionization on the distribution of the atoms in the low-pressure discharge was considered, with certain simplifications, in[15] for a planar discharge geometry.

2. Population of Excited Levels

The main mechanism of excitation of the working levels of an Ar II laser is stepwise excitation from the ion ground state[13,16], so that the expression for the population of these levels is

$$N_i^* = \frac{N_i \langle Q_{\text{exc}} v \rangle n_e}{A + \langle Q_{\text{dec}} v \rangle n_e}, \quad (2)$$

where N_i is the ion concentration in the ion ground state, A is the probability of radiative decay of the

[1)]The authors of[4] also indicate that the decrease of the gas density in the discharge of an Ar^+ laser, which they attribute to heating of the gas, can lead to a negative slope of the current-voltage characteristics.

level, and $\langle Q_{exc}v\rangle$ and $\langle Q_{dec}v\rangle$ are respectively the products of the level excitation cross section Q_{exc} and the decay cross section Q_{dec} by the electron velocity, averaged over the electron velocity distribution. The possible additional excitation of ionic levels by cascade population from the high-lying levels and stepwise process from the long-lived low-lying levels[13,16] also proceed during the first stage via the ion ground state, and can be disregarded in the qualitative treatment presented here, since they do not change the general dependence of the population on the electrical parameters of the plasma.

Comparing the dependence of n_e on J with the results of Fig. 5 (curve 2), we see that the increase of N_i^* at $J \gtrsim 150$ A is not connected with the increase of the charged-particle concentration, and is due only to the increase of T_e, which leads to an increase of $\langle Q_{exc}v\rangle$. The decrease of N_i^* after the maximum is reached is due to the decrease of n_e as the result of the quadratic dependence of the population, on n_e as given by (2) ($N_i \cong n_e$ under the experimental conditions). It should be noted that the decrease of N_a in the discharge with increasing current affects N_i in two ways. On the one hand, the decrease of N_a increases T_e, and this should increase the ionization as the result of the dependence of the ionization cross sections on the electron energy[14,10]. On the other hand, the ionization should decrease with decreasing N_a since the ionization rate is proportional to the number of ionized particles. The experimental results on Figs. 2 and 5 show that the second factor is predominant, and that the decrease of N_a with increasing J leads in final analysis to a decrease of the charged-particle concentration. The saturation of the intensity of the spontaneous emission can cause in principle also an increase in the number of decay-producing collisions, if

$$\langle Q_{dec}v\rangle n_e \gg A. \tag{3}$$

According to the available theoretical[16] and experimental[17] results, the largest Q_{dec} should be expected for electron collisions in which the excitation is transferred to low-lying ion levels, for which $\langle Q_{dec}v\rangle n_e \sim A$. Since n_e saturates with increasing J and then falls off, it becomes obvious that attempts to relate the current saturation of N_i^* with decay-producing collisions is inconsistent[2)]. Thus, the decrease of the working-level population with increasing current is due to the decrease in the numerator of (2), which represents the rate of level excitation (the pumping rate).

Let us turn to the results of measurements of the radial dependence of the spectral-line intensity. In the case of the current saturation of the ion lines (curve 3, Fig. 4b) the radial distribution of the intensity broadens in agreement with the considered mechanism of saturation of N_i^*, which should come into play primarily in the region where the gas has a minimum density at the discharge axis. The intensity of the atomic lines depends little on J up to ~ 200 A and decreases noticeably at the center of the tube (curves 1 and 2 of Fig. 4a). A similar behavior of the atomic lines was observed in a tube with a narrow discharge channel[18]. The increase of the intensity of the atomic lines at the center of the tube with increasing J (curve 3 of Fig. 4a) was not observed before at low values of p, and can be attributed to the peculiarities of the excitation of the atomic levels under the experimental conditions. The excitation of the upper level 5p of the line in question should occur in stepwise fashion, since this level is not coupled optically with the ground state of the atom and has a large stepwise excitation cross section[19]. We can therefore write for the population of this level

$$N_a^* = N_a \frac{\langle Q_{exc}^M v\rangle n_e}{A^M + \langle Q_{dec}^M v\rangle n_e} \frac{\langle Q_{exc} v\rangle n_e}{A + \langle Q_{dec} v\rangle n_e}, \tag{4}$$

where Q_{exc}^M, Q_{dec}^M and A^M are the excitation cross section, the decay cross section, and the total probability of the decay of the intermediate metastable level, which is independent of n_e. As noted in[18], relation (3) holds for the atomic levels, and therefore, according to (4) the population of the atomic levels does not depend on n_e and we can write

$$N_a^* = N_a F(T_e). \tag{5}$$

The function $F(T_e)$ is very sensitive to variation of T_e, since the integration carried out when the products Qv are averaged over the velocities begins with threshold energies near which the cross sections depend strongly on T_e, and the average electron energy is lower than the threshold excitation energies. The gas density decreases towards the discharge axis and $F(T_e)$ increases. The two quantities cancel each other in (5) and as a result N_a^* varies little along the radius. For the same reason, N_a^* depends little on J up to values ~ 200 A. Further increase of J, accompanied by a sharp decrease of N_a and by an increase of T_e, leads to an appreciable increase of the intensity of the atomic lines, especially in the axial part of the discharge. This points to a predominant role of the increase of $F(T_e)$ at currents $\gtrsim 200$ A and confirms indirectly the increase of T_e with increasing discharge current.

3. Generation Power

With the exception of the case of low gas pressure (curves 1 in Figs. 5 and 6), the generation power W increases strongly in comparison with the growth of the upper-level population. Thus, for curves 2 and 3, N_i^* changes only by $\lesssim 50\%$ when the current is varied from the generation threshold to the generation maximum, with N_i^* at the threshold quite large and comparable with N_i^* at the generation maximum in the case of lower p. This shows clearly that the populations of the upper working levels 4p increase more rapidly than the lower levels 4s when J increases from values near the generation threshold upwards. The given range of variation of J is characterized by an increase of T_e at constant n_e. The selective excitation of the 4p levels with increasing T_e can not be explained on the basis of the approximation wherein the excitation of the working levels proceeds only from the ion ground state, since the increase of T_e should lead to a simultaneous increase of $\langle Q_{exc}v\rangle$ for the 4p and 4s levels[13,16]. One can therefore expect an important role in the creation of the inverted population to be played by additional excitation mechanisms, for example, the contribution of the cas-

[2)]It should be noted that when n_e is increased, the decay-producing collisions can lead, according to (2), only to saturation but not to a decrease of N^*_i.

cade transitions from the 4d levels to the 4p levels which increases with increasing T_e[20], or the contribution of the direct excitation of the ionic levels from the atomic states. The important role of the additional mechanisms for the excitation of the 4p levels is evidenced also by the fact that the generation maxima for the individual lines occurred at somewhat differing currents. Thus, of the two generation lines (5145 and 4880 Å), the former was saturated at smaller values of J. To obtain a clear idea of the role of the different excitation mechanisms we need more accurate data on the excitation cross sections of the individual levels of each electronic configuration.

In spite of the lack of detailed data on the mechanism whereby inverted population is produced, the general picture of the dependence of W on the current, obtained on the basis of the results presented here, becomes perfectly understandable. The increase of J leads to an increase in the rate of excitation of the working levels. In the case of low pressures, T_e is high enough to produce inverted population, and therefore the increase of the rate of level excitation leads to a simultaneous increase of the inverted population, and after the threshold conditions are reached it leads to an increase of W. In this case, the dependences of N_i^* and W on J will be similar (curves 1). With increasing gas pressure, T_e decreases and at high values of p (curves 2—4) T_e becomes too low to ensure inverted population. The increase of the excitation rate with increasing current leads then to a growth of N_i^* and there is no generation. T_e increases simultaneously with increasing current, and when it becomes sufficient to produce inversion, an increase of the excitation rate is accompanied by an increase of W. During this stage of the generation development, the decrease of N_a is beneficial. Further increase of the current causes N_a to reach the limiting values, starting with which the rate of excitation of the ionic levels saturates as a result of a decrease of N_a, and this inevitably leads to saturation of W (the arrow at p = 1 mm Hg on Fig. 5 marks the position of the generation maximum). From the foregoing it becomes evident that W depends strongly on J at high values of p, since generation calls in this case for high values of J at which the required T_e must be obtained as a result of a considerable decrease of N_a, and which are quite close to the saturation currents.

The character of the current dependence of W and of the voltage U_t for a tube of 16 mm diameter, shown in Fig. 7, is similar to that for the tube with 11 mm diameter, and consequently the generation saturation in this tube is also due to the decrease of N_a in the discharge.

From the results in Figs. 6 and 7, and also from the results obtained with narrow tubes[1,6], we can see that the density of the generation-saturating currents decreases with increasing r. As a result, the obtained populations of the working levels, gains, and generation powers per unit volume are lower for wide tubes. Figure 8 illustrates the maximum gain G_m, measured under conditions close to current saturation[3)], as a function of the tube diameter. Within the limits of the

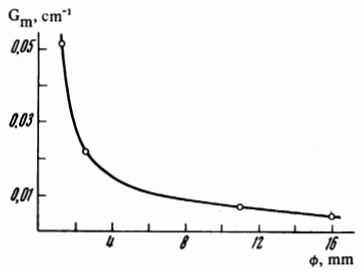

FIG. 8. Variation of the limiting values of the gain G_m with the tube diameter.

measurement errors (10%), G_m is inversely proportional to r. The power per unit discharge length increases with r. The laser efficiency increases simultaneously, since the electric power input EJ per unit discharge length is practically independent of r in the saturation regime.

Let us examine briefly other possible mechanisms for generation quenching. As already indicated, at $n_e \sim 10^{14}$ cm^{-3}, the disintegration of the upper working levels by electrons can come into play and decrease the inverted population. However, the decrease of the inversion as a result of the increase of n_e should, in accordance with (3), be simultaneously accompanied by an increase in the excitation rate of the working levels, which in turn leads to an increase of W. In the practically important case when the gain exceeds the threshold sufficiently, W turns out to be more critical to an increase in the excitation rate in a rather wide range of increasing n_e. An increase in the generation power of an argon laser with decreasing gain was experimentally observed in[1], and this question was considered theoretically by Odintsov[21], according to whom a decrease of W can be expected if $\langle Q_{dec} v \rangle n_e \sim A_l$, where A_l is the probability of radiative decay of the lower levels. Since A_l exceeds the decay probability of the upper working levels by more than one order of magnitude[9], the influence of the decay-producing electron collisions will be sufficient to quench the generation at $n_e \sim 10^{15}$ cm^{-3}. The cause of the generation quenching can be also an increase of the effective lifetime of the lower working levels, resulting from the dragging of their spontaneous emission, which can be approximately accounted for with the aid of the formula derived by Holstein[22]. Estimates based on this formula, using the values of T_i measured here and the spontaneous-decay probabilities calculated in[9], show that generation in a tube of 11 mm diameter can be quenched at $n_e \sim 6 \times 10^{14}$ cm^{-3}. This value exceeds by one order of magnitude the measured values of n_e in Fig. 2.

We see that the current saturation of W as a result the limitation on the excitation rate of the working levels, due to the decrease of N_a in the discharge, sets in much earlier than expected for the other saturation mechanisms. Consequently, if we succeed in lifting this limitation, then we can expect an appreciable increase of the efficiency and power of the generation at a fixed working volume, up to limits imposed by other generation-saturation mechanisms. Obviously, a simple increase of N_a in the discharge by increasing p in the system above the optimal value will not cause an increase of W, owing to the decrease of T_e, which leads in

[3)] In measurements with narrow tubes, symptoms of tube damage have appeared at saturation currents, so that we cannot exclude the possibility that the values given for small diameters are somewhat underestimated.

turn to a vanishing of the inversion. A slowdown in the decrease of N_a on the discharge axis with increasing current, without a substantial change of T_e, can be expected by using rapid flow of the gas across the tube, at velocities exceeding the thermal velocity of the atoms, $V \gtrsim \bar{v}_a$, for in this case the flow of atoms into the discharge will be increased by the increased atom velocity. This should shift the current saturation of W into the region of higher values, but serious obstacles can arise at the same time, owing to the strong drift of the discharge ions; alternately, there may be limitations of fundamental character, such as instability of the discharge.

CONCLUSION

The foregoing analysis of the behavior of the parameters of a strong-current plasma of a cw ion laser as functions of the pumping current shows that the limitations on the growth of W result from the decrease of N_a in the discharge, which limits the rate of excitation of the working levels. Such limits set in at lower pump-current densities in tubes of larger diameter, so that when the tube diameter is increased the per-unit output power and gain of the laser decrease. The output power per unit length and the efficiency in the current saturation regime increase with diameter within the limit ≤ 16 mm employed in this research. Obviously, at constant resonator losses, owing to the decrease of the gain with increasing diameter, it is advisable to increase the active length of the discharge simultaneously with the increase of the diameter. No investigations were made here of ion lasers with tubes of still larger diameter. One cannot exclude, for example, the possibility that an increase in the diameter, if not accompanied by a considerable decrease of n_e at saturation, will give rise to effects of dragging of the radiation from the lower working levels. However, it must be specially noted that the discharge instabilities described above can limit, independently of other factors, the increase of W and of the laser efficiency when the diameter is increased. Indeed, one can see already in Figs. 6 and 7 that the point at which instability sets in, and starting with which the maintaining voltage and the erosion of the tube increase, comes somewhat closer to the maximum generation in terms of the pump current with increase in diameter, and a subsequent slight increase of the diameter can produce instabilities in the discharge prior to the development of the maximum of W. These facts indicate that it is difficult to expect a considerable increase of W and of laser efficiency by using discharge tubes of larger diameter. Of great interest from the point of view of further increasing the output parameters of an ion laser is experimentation with gas drawn through the discharge at velocities $V \gtrsim v_a$.

The author is grateful to V. A. Grigor'ev for help with the measurements.

[1]V. I. Donin, Zh. Prikl. Spektrosk. **11,** 889 (1969); All-union Symposium on the Physics of Gas Lasers, Novosibirsk, July, 1969.
[2]V. I. Donin, Internat. Conf. on Lasers and Their Applications, Dresden, June, 1970.
[3]H. Boersch, J. Boscher, D. Hoder, and G. Schäfer, Phys. Lett. A **31,** 188 (1970).
[4]J. Boscher, T. Kindt, and G. Schäfer, Z. Phys. **241,** 280 (1971).
[5]V. I. Donin, V. M. Klement'ev, and V. P. Chebotaev, Zh. Prikl. Spektrosk. **5,** 388 (1966).
[6]V. I. Donin, Opt. Spektrosk. **26,** 298 (1969).
[7]V. I. Donin, Author's Certificate (Patent) No. 289458, Byull. Izobret. Tov. Znakov (1), ,(1971); Prib. Tekh. Eksp. (3), 161 (1971).
[8]S. É. Frish and O. P. Bochkova, Vestn. Leningr. Univ. **3,** 40 (1961).
[9]H. Statz, F. A. Horrigan, S. H. Koozekanani, C. L. Tang, and C. F. Koster, J. Appl. Phys. **36,** 2278 (1965); J. Appl. Phys. **39,** 4045 (1968).
[10]A. Von Engel, Ionized Gases, Oxford, U.P., 1965.
[11]V. L. Ginzburg and A. V. Gurevich, Usp. Fiz. Nauk **70,** 201 (1960) [Sov. Phys.-Usp. **3,** 115 (1960)].
[12]E. I. Asinovskiĭ and V. M. Batenin, Teplofiz. Vys. Temp. **6,** 966 (1968).
[13]V. F. Kitaeva, A. I. Odintsov, and N. N. Sobolev, Usp. Fiz. Nauk **99,** 361 (1969) [Sov. Phys.-Usp. **12,** 699 (1970)].
[14]L. Vriens, Phys. Lett. **8,** 260 (1964).
[15]A. Caruso and A. Cavaliere, Br. J. Appl. Phys. **15,** 1021 (1964).
[16]I. L. Beĭgman, L. A. Vaĭnshteĭn, P. L. Rubin, and N. N. Sobolev, Zh. Eksp. Teor. Fiz. Pis'ma Red. **6,** 919 (1967) [JETP Lett. **6,** 343 (1967)].
[17]N. M. Vladimirova, I. D. Kon'kov, R. E. Rovinskiĭ, and N. V. Cheburkin, Zh. Eksp. Teor. Fiz. **57,** 1506 (1969) [Sov. Phys.-JETP **30,** 813 (1970)].
[18]C. E. Webb, J. Appl. Phys. **39,** 5441 (1968).
[19]V. S. Krivchenkova and A. D. Khakhaeva, Opt. Spektrosk. **24,** 141 (1968).
[20]R. I. Rudko and C. L. Tang, J. Appl. Phys. **38,** 4731 (1967).
[21]A. I. Odintsov, Vestnik MGU, Ser.3 **11,** 391 (1970).
[22]T. Holstein, Phys. Rev. **83,** 1159 (1951).

Translated by J. G. Adashko
188